Nonlinear MHD Simulation of Current Drive by Coaxial Helicity Injection in Spherical Torus

Takashi KANKI[1], Masayoshi NAGATA[2], and Yasuhiro KAGEI[3]

[1]*Department of Maritime Science and Technology, Japan Coast Guard Academy, 5-1 Wakaba, Kure, Hiroshima 737-8512, Japan*

[2]*Department of Electrical Engineering and Computer Sciences, University of Hyogo, 2167 Shosha, Himeji, Hyogo 671-2201, Japan*

[3]*RIST, 2-4 Shirakata, Tokai, Ibaraki 319-1106, Japan*

(Received: 29 August 2008 / Accepted: 25 December 2008)

Nonlinear magnetohydrodynamic (MHD) simulations are carried out to investigate the dynamical behavior of spherical torus plasmas in coaxial helicity injection (CHI) and to provide the physical description of plasma flows and the relevant MHD relaxation phenomena. It is found from the simulation results that the toroidal flow is generated by the magnetic reconnection occurring at the X-point during the repetitive process of the non-axisymmetric magnetized plasmoid ejection from the magnetized coaxial plasma gun. The "bubble-burst" formation represented by the repetitive plasmoid ejection with the closed magnetic field lines is considered to be responsible for the CHI current drive.

Keywords: spherical torus, spheromak, coaxial helicity injection, current drive, MHD, simulation, plasma flow, magnetic reconnection, MHD relaxation, self-organization

1. Introduction

Coaxial helicity injection (CHI) [1] using a magnetized coaxial plasma gun (MCPG) has been successfully applied for both the formation and the sustainment of spherical torus (ST) including spheromak in the Compact Toroid Experiment (CTX) [2], the Flux Amplification Compact Torus (FACT) [3], the Sustained Spheromak Physics Experiment (SSPX) [4], the Helicity Injected Spherical Torus (HIST) [5], the Spheromak Experiment (SPHEX) [6] , the Helicity Injected Torus (HIT-II) [7], and the National Spherical Torus Experiment (NSTX) [8,9] devices, leading the attractive non-inductive plasma startup and current drive in low-aspect-ratio toroidal configurations. For instance, the CHI experiments in the HIST device have demonstrated discharges with up to toroidal current 150 kA and sustainment time 3-5 ms which is much longer than resistive decay time. However, the detailed physical mechanism of the current drive is not well understood. Recently, it is observed by the plasma flow measurements in the HIST device that the intermittent generation of the flow is correlated with the fluctuation on the electron density and toroidal current signals [10]. The repetitive merging of the magnetized plasma jet ejected from the MCPG may be responsible for the current sustainment, but its cause is not understood in detail. The purpose of this study is to investigate the dynamics of ST plasmas in the CHI systems by means of three-dimensional nonlinear resistive single-fluid magnetohydrodynamic (MHD) simulations [11,12], and provide the physical description of plasma flows and the relevant MHD relaxation phenomena.

2. Simulation Model

The numerical simulations are carried out in a three-dimensional full-toroidal cylindrical (r, θ, z) geometry, as shown in Fig. 1. The governing equations are the set of the nonlinear resistive MHD equations as follows:

$$\frac{\partial \rho \boldsymbol{v}}{\partial t} = -\nabla \cdot \rho \boldsymbol{v}\boldsymbol{v} + \boldsymbol{j} \times \boldsymbol{B} - \nabla p - \nabla \cdot \vec{\boldsymbol{\Pi}}, \tag{1}$$

$$\frac{\partial \boldsymbol{B}}{\partial t} = -\nabla \times \boldsymbol{E}, \tag{2}$$

$$\frac{\partial p}{\partial t} = -\nabla \cdot (p\boldsymbol{v} - \kappa \nabla T) - (\gamma - 1)(p \nabla \cdot \boldsymbol{v} + \vec{\boldsymbol{\Pi}} : \nabla \boldsymbol{v} - \eta j^2), \tag{3}$$

$$\boldsymbol{E} = -\boldsymbol{v} \times \boldsymbol{B} + \eta \boldsymbol{j}, \tag{4}$$

$$\boldsymbol{j} = \nabla \times \boldsymbol{B}, \tag{5}$$

$$T = \frac{p}{\rho}, \tag{6}$$

$$\vec{\boldsymbol{\Pi}} = \mu(\frac{2}{3}(\nabla \cdot \boldsymbol{v})\vec{\boldsymbol{I}} - \nabla \boldsymbol{v} - {}^{t}(\nabla \boldsymbol{v})), \tag{7}$$

author's e-mail: kanki@jcga.ac.jp

where ρ is the mass density, $\boldsymbol{v}$ is the fluid velocity, $\boldsymbol{B}$ is the magnetic field, and p is the plasma pressure. For simplicity, the conductivity κ, the viscosity μ, and the resistivity η are assumed to be uniform constant throughout the whole region. The ratio of specific heats γ is 5/3.

All variables are treated as a normalized form. Length, magnetic field, and mass density are normalized to the maximum length of the cylinder $L_0 = 0.5$ m, the strength of characteristic magnetic field $B_0 = 0.2$ T, and the initial mass density $\rho_0 = 5.0 \times 10^{19}$ /m^3, respectively. Under these normalization, the velocity and the time are normalized by the Alfvén velocity $v_A = 620$ km/s and the Alfvén transit time $\tau_A = 0.81$ μsec, respectively.

As shown in Fig. 1, we divide the simulation region in which the governing equations are solved into two-cylinders with a central conductor inserted along the symmetry axis. One is a gun region ($0.175 \le r \le 0.65$ and $0 \le z \le 0.5$) corresponding to the MCPG region. The other is a confinement region ($0.15 \le r \le 1.0$ and $0.5 \le z \le 2.0$). The insertion of a toroidal field current I_{tf} along the geometry axis inside the central conductor produces a vacuum toroidal field.

In order to solve the equations, we use the second-order finite differences method for the spatial derivatives, and the fourth-order Runge-Kutta method for the time integration. The grid numbers are chosen to be (N_r, N_θ, N_z) = (39, 64, 40) in the gun region and (N_r, N_θ, N_z) = (69, 64, 121) in the confinement region. Bias magnetic flux penetrates electrodes at the inner and outer boundaries of the gun region to drive the plasma current by applying the electric field. We use a perfect conducting boundary at the wall of the confinement region. The initial condition for the simulation is given by an axisymmetric MHD equilibrium which can be obtained by numerically solving a Grad-Shafranov equation derived from a force-free relation, $\nabla \times \boldsymbol{B} = \lambda \boldsymbol{B}$ under these boundary conditions. Here λ is the force-free parameter defined by $\lambda \equiv \boldsymbol{j} \cdot \boldsymbol{B} / B^2$. In the simulation, the mass density is spatially and temporally constant and no slip wall condition $\boldsymbol{v} = 0$ at all boundaries of the simulation region is assumed.

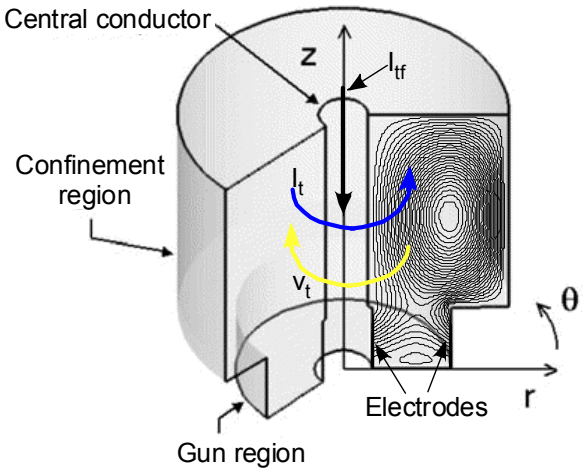

Fig. 1 Schematic view of the simulation region in cylindrical coordinate (r, θ, z).

3. Simulation Results

On the basis of the simulation results for the dynamics of ST plasmas in the CHI systems, the physical description of plasma flows and the relevant MHD relaxation phenomena are investigated. The parameters used in the simulation are the force-free parameter at the magnetic axis $\lambda_{axis} = 5.0$, $I_{tf} = 0$, and the safety factor at the magnetic axis $q_{axis} = 0.7$, corresponding to the spheromak configuration case. The poloidal flux contours with the axisymmetric MHD equilibrium used as the initial condition are shown in Fig. 1. Also, κ, μ, and η are assumed to be 1.0×10^{-3}, 1.0×10^{-3}, 2.0×10^{-4}, respectively.

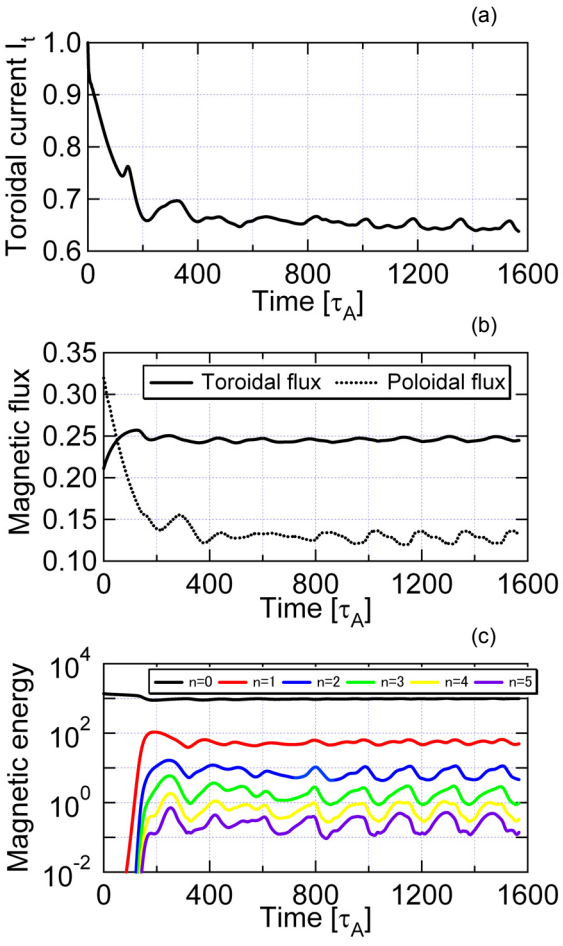

Fig. 2 Time evolutions of the toroidal current (a), the magnetic flux (b), and the magnetic energy for each toroidal Fourier mode n (c).

The toroidally symmetric radial electric field E_{inj} of 3.0×10^{-3} is always applied to the gap between gun electrodes during the simulation.

Figure 2 shows the time evolutions of the toroidal current I_t, the toroidal magnetic flux Ψ_t, the poloidal magnetic flux Ψ_p, and the magnetic energy W_{mag} for each toroidal Fourier mode n. As shown in Fig. 2(a), I_t is successfully sustained by overcoming resistive decay, and I_t, Ψ_t, Ψ_p, and W_{mag} have periodic oscillations after about $t = 800\,\tau_A$. The oscillations of I_t and Ψ_p are correlated very well, and Ψ_p reaches a maximum value at a peak of I_t.

Also, the oscillations of Ψ_p are out of phase with those of Ψ_t and W_{mag} for the $n \geq 1$ modes. This means the flux conversion from Ψ_t to Ψ_p which is related to the dominant n=1 oscillations. The plasma with this n=1 helical magnetic distortion rotates toroidally at frequency $f \approx 16$Hz calculated by the phase development of the toroidal current on the poloidal cross sections $\theta = 0$, $\pi/2$, π, and $3\pi/2$ rad. This plasma rotation due to $\boldsymbol{E} \times \boldsymbol{B}$ drift driven by the applied E_{inj} is in the opposite direction to I_t. This result is in agreement with observation in the HIST and other CHI experiments.

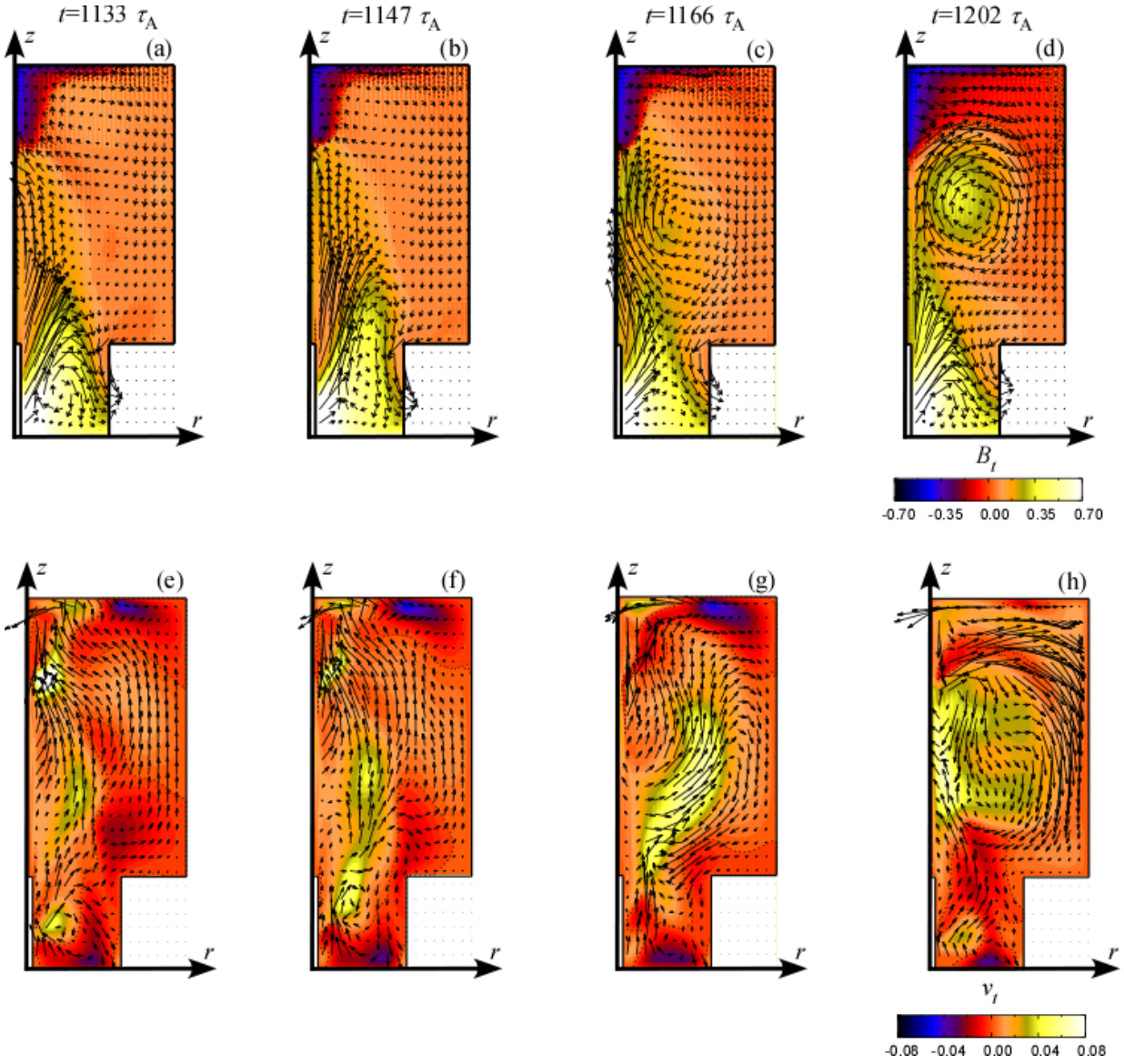

Fig. 3 Vector plots of poloidal magnetic field B_p and contours of toroidal field B_t on the poloidal cross sections $\theta = \pi/2$ rad at $t = 1133\ \tau_A$ (a), $t = 1147\ \tau_A$ (b), $t = 1166\ \tau_A$ (c), and $t = 1202\ \tau_A$ (d). The color on the toroidal magnetic field varies from black, blue, red, yellow to white as the magnetic field increases. Vector plots of poloidal flow velocity v_p and contours of toroidal flow velocity v_t on the poloidal cross sections $\theta = \pi/2$ rad at $t = 1133\ \tau_A$ (e), $t = 1147\ \tau_A$ (f), $t = 1166\ \tau_A$ (g), and $t = 1202\ \tau_A$ (h). The color on the toroidal flow velocity varies from black, blue, red, yellow to white as the flow velocity increases.

Figure 3 shows vector plots of the poloidal magnetic field B_p and contours of the toroidal field B_t, and vector plots of the poloidal flow velocity v_p and contours of the toroidal flow velocity v_t. The magnetized plasmoid is ejected from the gun region toward the confinement region, as shown in Figs. 3(a) and (b). When the poloidal gun current along the open magnetic field lines, i.e. the central open column surrounding the closed magnetic field lines increases, the critical current density gradient is reached. Then safety factor at plasma edge q_{edge} becomes 0.55 at t = 1166 τ_A, and the central open column violates the Kruskal-Shafranov kink stability criterion q > 1 [13]. The q calculation is based on the toroidally symmetric component of the magnetic field $q = d\Phi / d\Psi$, where Φ and Ψ are toroidal and poloidal magnetic flux, respectively. The n=1 kink mode of the central open column is destabilized, leading the helical distortion which is observed experimentally even if there is a conducting wall [10,14,15]. This kink mode is considered to be destabilized because the radius of the central conductor is small. As shown in Fig. 3(c), due to this physical process, the plasmiod with the n=1 helical distortion around the central conductor moves to the confinement region at t = 1166 τ_A, stretching the open field lines. As the result, the magnetic reconnection event occurs at the X-point near the gun muzzle, and then the toroidal flow ($v_t \approx 37$ km/s) is driven in the opposite direction to I_t, but in the same direction as the $\boldsymbol{E} \times \boldsymbol{B}$ plasma rotation, as shown in Figs. 1 and 3(g). This result is consistent with the flow observation in the HIST, HIT-II, and NSTX experiments. This magnetic reconnection activity results in the generation of the solitary closed poloidal field lines (magnetized plasmoid) at t = 1202 τ_A, as shown in Fig. 3(d). These closed field lines do not completely reach axisymmetric state because the helical distortion of the central open column rotates toroidally by the continuously applied E_{inj}. It is also seen from Fig. 3(h) that the magnetic configuration is in a partially relaxed state with a strong poloidal flow in the periphery region at t = 1202 τ_A. The magnetized plasmoid ejection is periodically performed, which is correlated with the generation of I_t and the n=1 oscillations. Therefore, the toroidal current is driven by the physical mechanism that the non-axisymmetric plasmoid is repetitively provided by the MCPG.

4. Conclusions

We have investigated the dynamics of ST plasmas in the CHI systems by means of the nonlinear MHD simulations, and provided the physical description of plasma flows and the relevant MHD relaxation phenomena. It is found from the simulation results that the toroidal flow is generated by the magnetic reconnection occurring at the X-point during the repetitive process of the non-axisymmetric magnetized plasmoid ejection from the gun region. The periodicity of this plasmoid ejection is correlated with the generation of the toroidal current and the n=1 oscillations. The toroidal flow ($v_t \approx 37$ km/s) driven by the magnetic reconnection is the opposite direction to the toroidal current, but in the same direction as the $\boldsymbol{E} \times \boldsymbol{B}$ drift flow. This result is consistent with the flow observation in the CHI experiments. The "bubble-burst" formation represented by the repetitive plasmoid ejection with the closed magnetic field lines is considered to be responsible for the CHI current drive.

In the future, we will investigate the dynamo electric field produced by the nonlinear development of the n=1 helical kinked central open column and its relevant generation of the plasmoid and the toroidal current.

References

[1] T.R. Jarboe, Fusion Techol. **15**, 7 (1989).
[2] S.O. Knox *et al*., Phys. Rev. Lett. **56**, 842 (1986).
[3] M. Nagata *et al*., Phys. Rev. Lett. **71**, 4342 (1993).
[4] H.S. McLean *et al*., Phys. Rev. Lett. **88**, 125004 (2002).
[5] M. Nagata *et al*., Phys. Plasmas **10**, 2932 (2003).
[6] P.K. Browning *et al*., Phys. Rev. Lett. **68**, 1722 (1992).
[7] A.J. Redd *et al*., Phys. Plasmas **15**, 022506 (2008).
[8] R. Raman *et al*., Phys. Plasmas **14**, 056106 (2007).
[9] M. Nagata *et al*., Plasma and Fusion Res. **2**, 035 (2007).
[10] M. Nagata *et al*., "Experimental and Computational Studies of MHD Relaxation Generated by Coaxial Helicity Injection in the HIST Spherical Torus Plasmas", 22nd IAEA Fusion Energy Conference, October 13-18, 2008, EX/P6-7.
[11] Y. Kagei *et al*., J. Plasma Fusion Res. **79**, 217 (2003).
[12] Y. Kagei *et al*., Plasma Phys. Control. Fusion **45**, L17 (2003).
[13] P.M. Bellan, *Fundamentals of Plasma Physics* (Cambridge University Press, Cambridge, 2006) p.382.
[14] R. Duck *et al*., Plasma Phys. Control. Fusion **39**, 715 (1997).
[15] D. Brennan *et al*., Phys. Plasmas **6**, 4248 (1999).